SOILS AND FOUNDATIONS Vol. 47, No. 5, 873–885, Oct. 2007
Japanese Geotechnical Society

COMPARATIVE STUDY ON THE BEHAVIOR OF ENCASED STONE COLUMN AND CONVENTIONAL STONE COLUMN

MALARVIZHI[i] and ILAMPARUTHI[ii]

ABSTRACT

Stone columns, one of the most commonly used soil improvement techniques, have been utilized worldwide to increase bearing capacity and reduce total and differential settlements of structures constructed on soft clay. Stone columns also act as vertical drains, thus speeding up the process of consolidation. However, the settlement of stabilised bed is not reduced in many situations for want of adequate lateral restraint. Encasing the stone column with a geogrid enhances the bearing capacity and reduces the settlement drastically without compromising its effect as a drain, unlike a pile. The behavior of the encased stone column stabilized bed is experimentally investigated and analysed numerically. In the numerical analysis, material behaviour is simulated using Soft Soil, Mohr Coulomb and Geogrid models for clay, stone material and encasement respectively and is validated with experimental results. The parametric study carried out on varying the L/D ratio (L = length of the column; D = diameter of the column) of column, stiffness of geogrid and angle of internal friction of stone material gives a better understanding of the physical performance of the encased stone column stabilized clay bed.

Key words: coupled FE analysis, geogrid encasement, settlement reduction ratio, soft clay, stone column (**IGC**: E2/E13/E14/K3/K14/M9)

INTRODUCTION

Soft clay deposits are geologically very young deposits, widely spread along the coastal plains all over the world. These deposits pose a major problem to geotechnical engineers because of low shear strength and high compressibility. Ground improvement by the stone column technique overcomes these problems by reducing the total settlement under load and by speeding up the process of consolidation. Stone columns derive their axial capacity from the passive earth pressure developed owing to bulging of columns and resistance to lateral deformation under superimposed loads. Stone columns act as drains and accelerate the primary consolidation. However, when used in soft clay, stone columns have certain limitations. The interface layer between the clay and the stone column is a mixed layer of clay and stones, which prevents the effective drainage (i.e. clogging of drain). Materials (stone pieces) of stone column get into the surrounding soil due to inadequate lateral confinement, particularly at depths closer to the ground. This effect is severe in soft clays, thus causing the stabilized bed to settle excessively. To overcome these limitations, stone columns are encased using geosynthetics. In the encased stone column, hoop stresses develop in the encasement, which act as an elastic tube, and provide the necessary restraint to the stone column. Further, encasement prevents intermixing of clay and column material (stone), thus drainage of column is not affected.

The theory of load transfer, estimation of ultimate bearing capacity and prediction of settlement of stone column was developed over a period of four decades by numerous researchers (Greenwood, 1970; Hughes and Withers, 1974; Aboshi et al., 1979; Balaam and Poulos, 1983; Priebe, 1976; Van Impe and De Beer, 1983; Madhav et al., 1994, Boussida and Hadri, 1995). Mitchell and Huber (1985) have shown that stone columns reduce the settlement significantly. Lee and Pande (1998) proposed a numerical model to analyze elastic as well as elastoplastic behavior of foundation bed reinforced with stone columns. To understand the mechanism of encased stone column, Deshpande and Vyas (1996) conducted test on encased stone column and demonstrated that the elastic behaviour of encasement induces hoop compression that results in an upward thrust releasing part of column load, and reduces lateral pressure to the surrounding clay. Katti et al. (1993) proposed a theory for improvement of soft ground using stone columns with geosynthetic encasing based on particulate concept. Sivakumar et al. (2004) have conducted two series of triaxial tests on sand columns of 32 mm diameter, with and without geogrid encasing of different lengths and concluded that the columns longer than five times the diameter do not contribute to the increase in load-carrying capacity. Bauer

[i] Research Scholar, Division of Soil Mechanics and Foundation Engineering, Anna University, India (malar_sn@yahoo.com).
[ii] Professor, ditto.
The manuscript for this paper was received for review on September 1, 2006; approved on May 29, 2007.
Written discussions on this paper should be submitted before May 1, 2008 to the Japanese Geotechnical Society, 4-38-2, Sengoku, Bunkyo-ku, Tokyo 112-0011, Japan. Upon request the closing date may be extended one month.

and Nabil (1996) carried out triaxial tests on two types of granular material with and without the geogrid sleeves. They reported that the granular material packed within the cylindrical sleeve, increased the stiffness of the system considerably. Adayat and Hanna (2005) used encapsulated stone to improve collapsible soils. A few studies have reported the application of geotextile encased stone columns (Short et al., 2004; Alexiew et al., 2005; Raithel et al., 2005), yet the proper understanding of the behaviour of the columns is limited.

The scope of this study is to understand the behavior of encased stone columns in soft clay and to bring out the parameters which play dominant role in load sharing and settlement reduction in the encased stone column stabilized bed. With this as objective, laboratory tests were carried out on scaled down models approximately 1/20 size of prototype. The encased stone column stabilized models were also analyzed using PLAXIS FEM code. An attempt was made to include non-linear behavior of soil and column material. The results of numerical analyses were compared with the experimental results of this study as well as with the earlier theories and experiments published. An extensive parametric study was carried out to understand the influence of L/D ratio of column, the stiffness of geogrid and the angle of internal friction of stone material on settlement reduction of the stabilized clay bed.

Table 1. Properties of clay selected for this study

Specific gravity	2.68
Liquid limit	55%
Plastic limit	18%
Plasticity index	37%
Clay	65%
Silt	27%
Unified Soil Classification	CH
Compression Index	0.75

Table 2. Properties of the stone chips

Confining pressure, σ_3 (kN/m^2)	Initial tangent modulus, E_i (kN/m^2)
50	2857
100	4200
200	13300
Angle of shearing resistance	46°

Table 3. Specifications of the nets used

Net Id.	Wt. gm/m^2	Aperture size	E_s (kN/m)
net1	260	Diamond 1 mm × 1 mm	15
net2	475	Square 4 mm	40
net3	730	Diamond 8 mm × 6 mm	60

EXPERIMENTAL INVESTIGATION

Selection of Clay

Clay with high compressibility was required for this study. Therefore, the soil samples were collected from different locations and tested for their index properties. The soil collected from Tharamani area, near Chennai, which is on the southeast coastline of India is geologically young and is highly compressible ($C_c = 0.75$). The test for particle size distribution showed that the fines are 92% out of which clay fraction alone was 65%. The other properties of the soil are presented in the Table 1 and the soil is classified as CH type. Moreover, stone column technique is in practice to support large storage tanks in this deposit. Therefore, the clayey soil of Tharamani area is considered suitable for the research study.

Properties of Stone Column Material

Stone column of 30 mm diameter was formed using granite stone chips of particle sizes varying from 2 to 6.35 mm. The maximum particle size (6.35 mm) of the stone used is 1/5 diameter of the column, which is slightly higher than the recommended guidelines of Nayak (1983). The stone column material was well graded and found to have ϕ value of 48° at a unit weight of 16 kN/m^3 as obtained from the large shear box tests. The initial tangent moduli of the column materials were determined at the unit weight of 16 kN/m^3 under three confining pressures and the values are presented in Table 2 along with the angle of shearing resistance. The angle of shearing resistance obtained through triaxial test is 2° less than the direct shear test value. This difference is attributed to plane strain condition of direct shear test. However, the difference is marginal (<5%), therefore ϕ value of direct shear test was used in the analysis.

Materials Used for Encasement

Three different materials were used for encasement, which are (i) Nova curtain (net1), commercially known as mosquito net, (ii) Netlon square mesh (net2) known as the garden net and (iii) Netlon CE121, known as geonet (net3). Cylindrical tubes were stitched using these materials for encasing the stone columns. The connection of the cylindrical tube was made with high strength polyester cord. The properties of the nets (manufacturer's data) and their initial tensile modulus (E_s) obtained from the tensile strength tests (ASTM D6637) are presented in Table 3. Columns encased using net2 and net3 were additionally covered with a thin geotextile to allow drainage without clogging of soil into the aperture and to prevent slipping of stone particles smaller than the aperture opening. The geotextile was arranged in such a way that it would not contribute either to the vertical or lateral stiffness of the encased stone column.

Preparation of Soft Clay Bed

The air-dried clayey soil was mixed with required quantity of water to achieve a consistency index of 0.1 at a water content of 52%. Initially the soil was thoroughly mixed with the water and kept covered for 48 hours to ensure uniform consistency. After 48 hours of hydration, the soil was mixed and kneaded well and checked for

moisture content. Loss of water, if any due to evaporation, was compensated before forming the bed. Care was taken to avoid entrapment of air while preparing the bed. However, each layer of clay was tapped gently using a wooden plank to remove entrapped air, if present.

Formation of Stone Column

The centre of the cylindrical tank was properly marked, a casing of required diameter was placed, and then clay bed was formed in layers around the casing. The stones were carefully charged into the casing and compacted using 12 mm diameter rod to achieve a density of 16 kN/m^3. At the end of compaction of each layer, the casing tube is withdrawn to a certain level and stone is charged and compacted. This procedure is repeated until the full length of column is formed.

Formation of Encased Stone Column

For the encased stone column, geogrid/net was stitched into a tube of required diameter as explained earlier and inserted along with the casing. The stones were compacted in the same way as it was done in the case of the stone column.

The bed thus prepared was loaded with a seating pressure of 2.5 kN/m^2 to the entire area of the bed for 24 hours to obtain uniform bed, which also ensured proper contact between clay and encased stone column. The test carried out after 24 hours of preparation of the bed also ensured gain in the strength of disturbed clay.

Experimental Setup for the Load Test

Tests were conducted on a single stone column of diameter 30 mm for various L/D ratios (L = length of the column; D = diameter of the column) on a standard loading frame as a stress-controlled test. The loading arrangement is shown in Fig. 1. The size of the tank was 300 mm in diameter and 300 mm in height, (H). The equivalent diameter of the tributary area for a spacing of $2D$ in a square pattern is $2.3D$ (≈ 1.13 times spacing). So the stabilized clay bed is loaded through a steel rigid circular plate of diameter $2.3D$. The lateral dimension of the tank was chosen to be such that the minimum free distance between the periphery of the column and the side of the tank does not interface with the failure wedge.

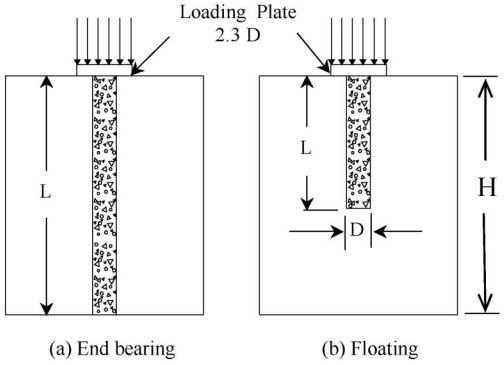

Fig. 1. Schematic arrangement of stone columns

Meyerhof and Sastry (1978) established that the failure zone extends over a radial distance of about 1.5 times the diameter from the periphery of column. Load tests were conducted on clay beds stabilized with stone column and encased stone column independently by loading the plate in 8 to 15 equal load increments. The cumulative equal increments of load thus applied were maintained constant for a period of one hour. During this one-hour period, settlements were recorded at an interval of 10 minutes using two sensitive dial gauges resting at diametrically opposite ends of the plate.

MODELS USED FOR NUMERICAL STUDY

Numerical analyses of the model tests were accomplished by the PLAXIS finite element software. Elastoplastic behaviour of stone-column is modeled by Mohr-Coulomb yield criterion employing a non-associated flow rule. The non-associated flow rule in this case has a significant meaning in the sense that the dilation of the stone-column on shearing can be represented by adjusting the dilatancy angle.

The non-linear behaviour of clay is represented by the modified critical state model, the Soft soil model. The Soft soil model is extensively described in Vermeer and Brinkgreve (1998), which is similar to the modified Cam clay model, without softening behaviour. The Soft Soil model is meant for primary compression of near normally-consolidated clay-type soils. Some features of the Soft-Soil model are:

- Stress dependent stiffness (logarithmic compression behaviour).
- Distinction between primary loading and unloading-reloading.
- Memory for pre-consolidation stress.
- Failure behaviour according to the Mohr-Coulomb criterion.

Soft Soil model requires the following material constants: modified compression index, λ^*, modified swelling index, κ^*, cohesion, c′, friction angle, ϕ, dilatancy angle, ψ, poison's ratio and k_0, coefficient of lateral stress in normal consolidation. The difference of this model from the Modified Cam clay model is that it is a function of volumetric strain instead of void ratio. The parameter λ^* is the modified compression index, which determines the compressibility of the material in primary loading given by Eq. (1). It is assumed that there is a logarithmic relation between the volumetric strain, ε_v, and the mean effective stress, p', which can be formulated as:

$$\varepsilon_v - \varepsilon_v^0 = -\lambda^* \ln\left(\frac{p'}{p^0}\right) \tag{1}$$

ε_v^0 is the initial volumetric strain corresponding to the initial stress p^0. The parameter κ^* is the modified swelling index, which determines the compressibility of the material in unloading and subsequent reloading. Note that κ^* differs from the index κ as used by Burland (1965) in Modified Cam clay model. The ratio λ^*/κ^* is, however, equal to Burland's ratio λ/κ. The parameters

λ^* and κ^* are obtained from the one-dimensional compression test. A relationship exists with the internationally recognized parameters for one-dimensional compression, C_c given by Eq. (2).

$$\lambda^* = \frac{C_c}{2.3(1+e)} \tag{2}$$

The factor 2.3 is obtained from the ratio between the logarithm of base 10 and the natural logarithm. The ratio λ^*/κ^* $(=\lambda/\kappa)$ ranges, in general, between 3 and 7. The elastic behaviour is described by Hooke's law and it relates linear stress dependency on the tangent bulk modulus as in Eq. (3).

$$K_{ur} \equiv \frac{E_{ur}}{3(1-2\nu_{ur})} = \frac{p'}{\kappa^*} \tag{3}$$

The suffix 'ur' stands for unloading reloading. Neither the elastic bulk modulus, K_{ur}, nor the elastic Young's modulus, E_{ur}, is used as an input parameter. Instead, ν_{ur} and κ^* are used as input constants for the part of the model that computes the elastic strains. The poisson's ratio used is the well known pure elastic constant rather than a pseudo-elasticity constant as used in the Mohr Coulomb model. It is also possible to specify undrained behaviour in an effective stress analysis using effective model parameters. The presence of pore pressures in a soil body, usually caused by water, contributes to the total stress level. According to Terzaghi's principle, total stresses σ can be divided into effective stresses σ' and pore water pressures σ_w, given by $\sigma_{xx} = \sigma'_{xx} + \sigma_w$; $\sigma_{yy} = \sigma'_{yy} + \sigma_w$. However, water is supposed not to sustain any shear stress, and therefore the effective shear stresses are equal to the total shear stresses $(\sigma_{xy} = \sigma'_{xy})$. Cohesion and angle of internal friction are the effective stress parameters obtained from the drained triaxial test. The permeability, k is calculated from the c_v obtained from the consolidation test.

Application of these two material models were verified with the published results of Lee and Pande (1998) wherein Cam clay and Mohr Coulomb models were used to analyze the stone column stabilized clay bed. The result of numerical study compares reasonably well with both the experimental and the numerical results of Lee and Pande (Fig. 2). Therefore, these two models were adopted for further analysis.

The properties of the clay and stone are presented in Table 4. These properties of stone material and clay were determined through triaxial tests conducted on specimens in the laboratory as per ASTM D4767. When the stone material alone was tested at low confining pressures and the volume change was measured through drained triaxial tests on stone specimens of 75 mm diameter, the dilatancy was observed to be 26°. However, the dilatancy of the stone material was found to be only 4° when it was packed within the geogrid encasing. The initial tangent modulus obtained from triaxial test on the encased stone column was used for the stone material within the encasement to incorporate the initial confinement effect offered by the geogrid encasement.

The geogrid was modeled as linear elastic continuum element whose axial stiffness was taken as the initial tangent modulus, obtained from the tension test. The initial tensile modulus, (EA) of the geogrids (ratio of the axial

Table 4. Parameters used for material modeling

Parameter	Clay	Stone column	Encased Stone column
Model	Soft soil	Mohr Coulomb	Mohr Coulomb
E [kPa]	Not reqd.	2500	9000
ν	0.2	0.3	0.3
γ [kN/m^3]	11	16	16
Φ' [°]	24	48	48
c' [kPa]	6	0.1	0.1
ψ [°]	0	26	4
k (m/day)	$5.94e^{-4}$	1	1
λ^*	0.136	Not reqd.	Not reqd.
κ^*	0.054	,,	,,
e_o	1.42	,,	,,

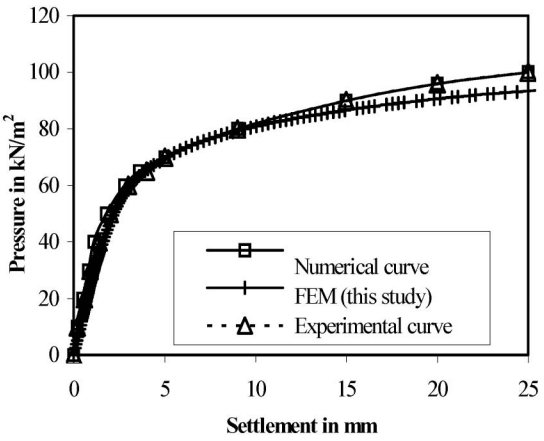

Fig. 2. Validation of FEM with Lee and Pande (1998)

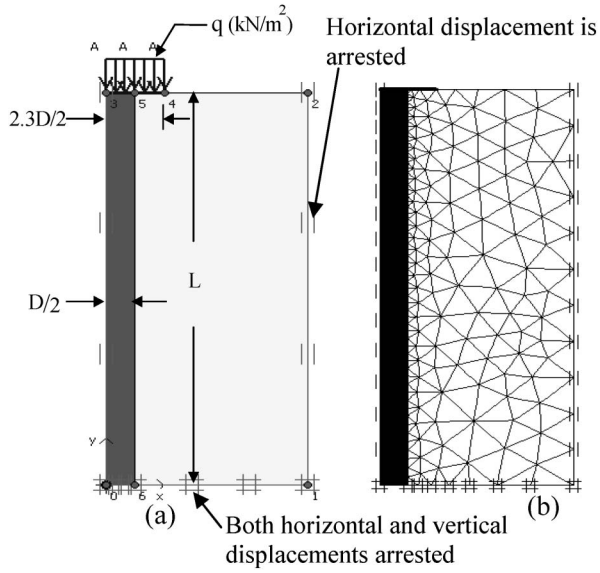

Fig. 3. Typical FE model of clay bed and column

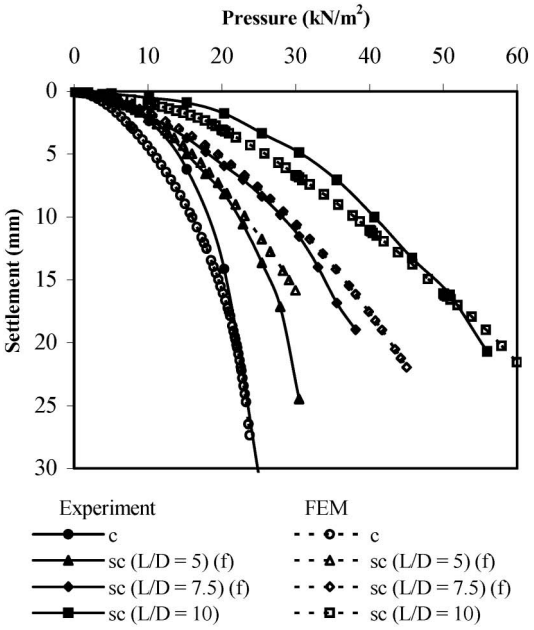

Fig. 4. Load vs. Settlement curve of stone columns

force per unit width and the axial strain) obtained from the tension tests on net1, net2 and net3 (Table 3) were incorporated in the model. Axisymmetric finite element analysis was carried out since studies were on single column stabilized bed under symmetric load. A typical finite element idealization of the laboratory model is shown in Fig. 3(a) wherein numbers (0–6) indicate the sequence followed in creating geometric boundaries. In PLAXIS finite element code, mesh generation is automatic with 6 or 15 noded triangular elements (Fig. 3(b)). Fifteen noded triangular elements were chosen for meshing. The nodes at the vertical boundaries were not allowed to displace horizontally but allowed to undergo vertical displacement whereas for the nodes at the bottom surface, both horizontal and vertical displacements were arrested.

RESULTS AND DISCUSSION

Load-Settlement Response of Clay and Stone Column Stabilised Beds

In Fig. 4, the load-settlement behavior of soft clay bed (c) and stone column stabilized bed (sc) are compared. The settlement of clay bed increases with increase in load and shows a continuous deformation (settlement) at a more or less constant load (pressure). This response typifies the behaviour of highly compressible clay. The load-settlement response of stone column stabilized bed also shows similar trend but for a given load, the settlement is less and is decreased with increase in column length. The settlement is lesser for end bearing column than floating columns (f) for a given consistency and thickness of clay bed. Further, the rate of increase of settlement decreases with column length. Thus, the load carrying capacity and stiffness of clay bed are improved due to stone column

Table 5. Load resistance of stone column stabilized bed at 10 mm settlement

Column type	Expt. (kN/m²)	FEM (kN/m²)
Clay	18	16
sc ($L/D=5$)	22	23
sc ($L/D=7.5$)	27	28
sc ($L/D=10$)	40	38

stabilization and the length of column plays a significant role in settlement reduction. For an applied pressure, the settlement observed is less when the stone column length is increased. The higher the L/D ratio is, the lesser the settlement.

The load-settlement curves obtained through FEM analyses show almost similar trend as observed in experiments and are compared in Fig. 4. In case of virgin clay, the load-settlement behaviour is obtained using Soft soil model, which compares well with the experimental curve. The load-settlement response for stone column stabilized beds (both floating and end bearing) using Soft soil and Mohr coulomb models for clay and stone column respectively are compared with the corresponding experimental curves. The comparison is extremely good for floating stone columns and for the end bearing columns, the difference in load is around 5% for a given settlement. The loads for 10 mm settlement are presented in Table 5. Experimental results are found to agree very well with the FEM results. The increase in carrying capacity is of the order of 2.2, 1.5 and 1.2 times that of the untreated bed for columns with L/D ratio 10, 7.5 and 5 respectively.

Behavior of Conventional Stone Column

The deformed shape of the stone column stabilized bed shows considerable bulging as shown in Fig. 5. The bulging was observed both from the numerical and experimental investigations. From numerical studies, it was found to extend from the column head to a depth varying between 2.5 and 6 times the column diameter. The radial deformation, x (expansion of outer face of the column in the radial direction due to load on the column), in other words bulging, increased gradually with the pressure as shown in Fig. 6 and the bulging was maximum at a depth of $1.75D$ from the top. It was observed to be 6.7 mm (i.e. $0.22D$) for a vertical pressure of 60 kN/m². The bulging of stone column was also measured by exhuming the stone column, which was grouted at the end of the test. Maximum bulging was seen at $1.5D$ depth of the column, and compared well with the numerical analysis.

Greenwood (1970) postulated that the stone column resists the vertical load by the passive resistance offered by the surrounding soil to the bulging of column and that the depth of bulge is around 2 times the pile diameter. However, Hughes and Withers (1974), showed that the critical length is 4 times the pile diameter, in case of bulging failure. Thus, observations made in this study agree well with the findings of earlier investigators.

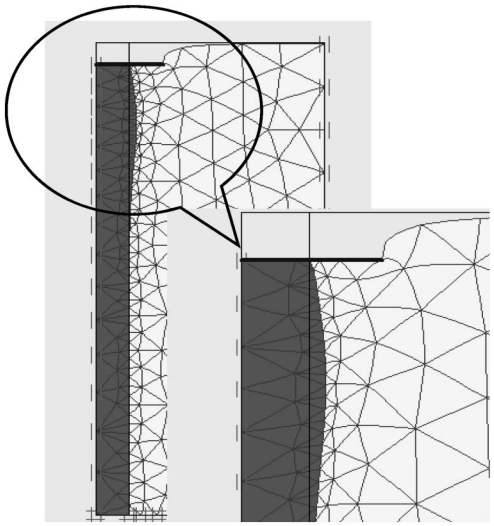

Fig. 5. Deformed shape of stone column

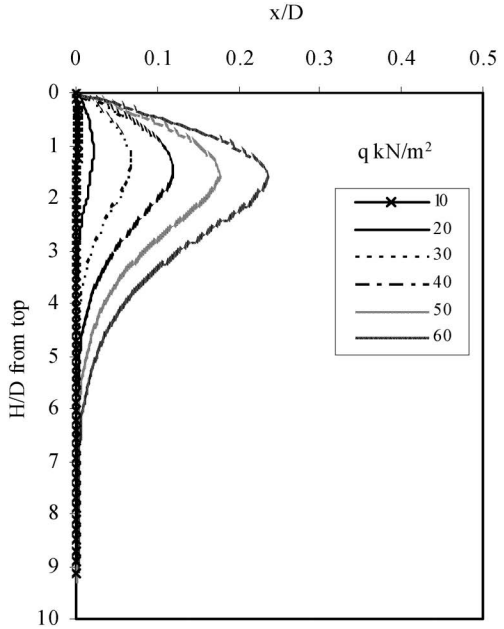

Fig. 6. Bulging of stone column with pressure

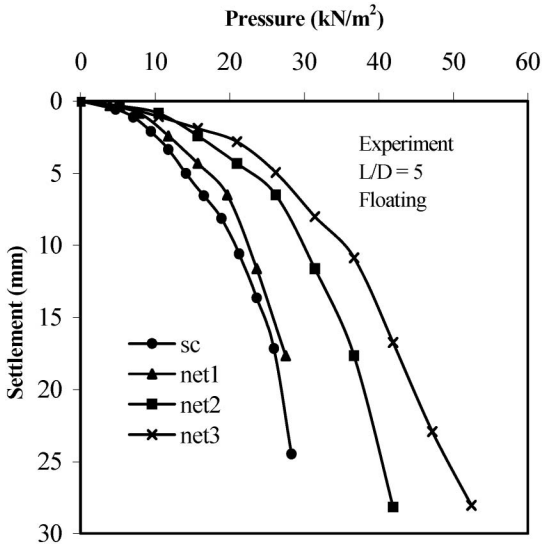

Fig. 7(a). Load vs. Settlement of encased columns

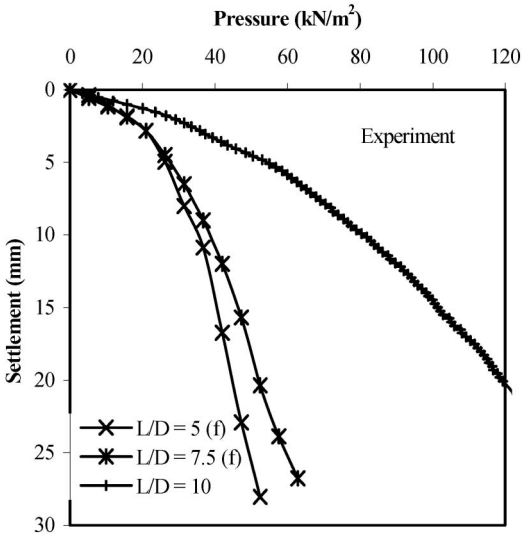

Fig. 7(b). Load vs. Settlement response of floating and end bearing columns with encasement (net3)

Load-Settlement Response of Clay Bed Stabilized with Encased Stone Column

The load-settlement responses of stone columns encased with three different nets (net1, net2 and net3) for different L/D ratios are presented in Fig. 7(a), 7(b) and 7(c). In all these cases, the shape of load-settlement curve is almost similar to clay bed stabilized with stone column. These curves show higher resistance against the load and the rate of increase of settlement is less while comparing with stone column stabilized bed.

In Fig. 7(a), the effect of stiffness of reinforcement is compared with stone column for a floating column arrangement ($L/D=5$). As stated earlier the characteristic behaviour of stabilized bed is not affected but the bed stiffness is increased with the stiffness of the encasing material and overall load carrying capacity is also increased. The effect of length of column on the load resistance is compared in Fig. 7(b) for the columns stabilized with net3. The bearing pressure increases as the length increases, but the improvement is not significant when the columns are floating (f). The improvement is significant when the columns are end bearing.

The load settlement response of end bearing columns ($L/D=10$) is presented in Fig. 7(c) and compared with the response of FEM analysis. For a particular settlement, the load carried by the encased stone column is higher than the stone column. The tensile strength of net1 is very small therefore the load capacity is not significant. The net3 column offered higher resistance than net2 column for a given settlement of the stabilized bed. Table 6 summarises the load for 10 mm settlement for the beds stabilized with encased stone column. The bearing pres-

Table 6. Load resistance of stabilized beds at 10 mm settlement in kN/m²

Column	$L/D=5$	$L/D=7.5$	$L/D=10$
sc	21	27	40
net1	22.5	29	45
net2	30	32	63
net3	35.5	39	81

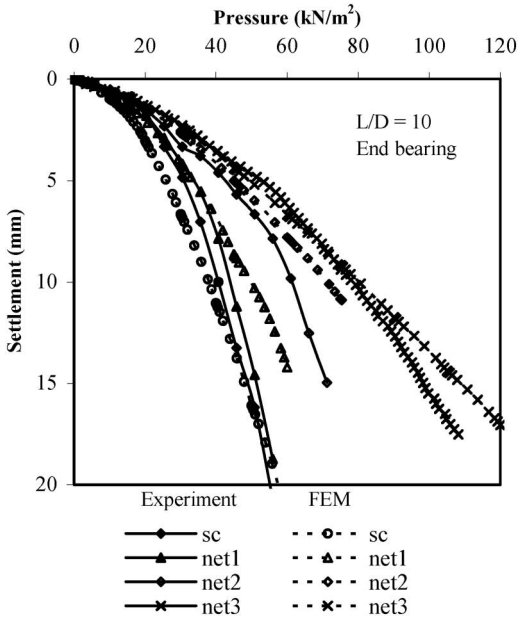

Fig. 7(c). Comparison of load vs. settlement response between experiment and FE analysis

sure for floating columns ($L/D=5$) at 10 mm settlement is 21 kN/m², 22.5 kN/m², 30 kN/m² and 35.5 kN/m² for stone column, net1 column, net2 column and net3 column respectively. Thus, the respective capacities are 1.05, 1.4 and 1.7 times the stone column stabilized. Similarly, for floating stone column with L/D ratio of 7.5, the carrying capacities of net1, net2 and net3 columns are 1.07, 1.2 and 1.4 times the capacity of the stone column stabilized bed. The bearing pressures at 10 mm settlement are 45 kN/m², 63 kN/m² and 81 kN/m² for net1, net2 and net3 encased end bearing columns respectively. The increase in carrying capacity is of the order of 1.1, 1.6 and 2.0 times that of the stone column stabilized bed. The end bearing columns performed better than the floating columns. In all the cases, the increase in capacity is more than two times the capacity of respective floating columns with $L/D=5$. In all the cases, it was found that the load capacity of the stabilized bed increases in proportion to the increase in the stiffness of geogrid material.

The load-settlement response of encased stone column stabilized beds is obtained using FEM, wherein encasement (geogrid) is modeled as linear elastic material. The FEM curves showed almost similar response as that of the experimental curves (Fig. 7(c)). Thus the material models viz. Soft soil, Mohr coulomb and geogrid model used in this study for clay, stone column and encasement

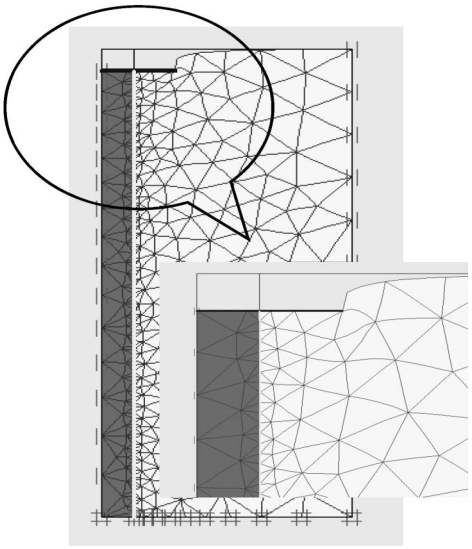

Fig. 8. Deformed shape of encased stone column

respectively predicted their behaviours reasonably well.

Mechanism of Encased Stone Column

A typical deformed shape of encased stone column stabilized bed, from the finite element analysis is shown in Fig. 8. When the encased stone column is subjected to vertical load, the column material tends to dilate and induces lateral pressure. If the resistance offered by the surrounding soil is not sufficient to restrain bulging especially in soft soil, the column may fail due to excessive bulging, in which case the lateral confining effect is offered by the encasing material.

Stone material dilates and lateral strain in the stone column induces hoop tension in the encasement, which results in radial compression in stone column. The hoop tension developed depends on the stiffness of geogrid and it offers a passive resistance to the stone column, which is otherwise offered by the surrounding soil. The lateral pressure thus developed results in an upward thrust (Deshpande and Vyas, 1996).

The stress transferred to the stone thus increases, which in turn reduces the load on the clay. Despite the increase in stress in the column, bulging of stone column was reduced significantly. The settlement of stabilized bed was much less for the same magnitude of pressure. For a pressure of 60 kN/m², the maximum horizontal deformation or maximum bulging was found to be 0.73 mm, 0.24 mm and 0.17 mm in net1, net2 and net3 respectively as against 6.7 mm in the conventional stone column. The hoop forces mobilized in the geogrid reduced the bulging. The mobilization of hoop forces in the geogrid increases with applied load. The stiffer the geogrid is, the greater the hoop stress is developed. Maximum hoop force is developed at the depth around 1D of the encasement, which is shown in Fig. 9. For higher pressures, hoop forces are mobilized over the entire length of the encasement.

Stress Concentration in Columns

Stress concentration ratio is defined as the ratio of axial stress experienced by the column to the vertical stress component sustained by the soil for the same applied pressure. Due to the increased stiffness of the stone column, stress concentration is more on the column than in the surrounding soil. When the stone column is encased, the stress concentration ratio in the stone further increases as shown in Fig. 10 and the magnitude of increase depends on the stiffness of material used for the encasement. The stress concentration ratio on the stone column is 8.4 for an applied pressure of 20 kN/m^2 and reduced to 3.7 for 60 kN/m^2. From Fig. 10, it is observed that the stress concentration ratio increased proportionally with the stiffness of geogrid encasement. For a pressure of 120 kN/m^2, the stress concentration ratio of the encased stone column was observed to be 14, 41 and 54 for net1, net2 and net3 respectively which is in proportion to their initial tensile modulus of 15 kN/m^2/m, 40 kN/m^2/m and 60 kN/m^2/m respectively.

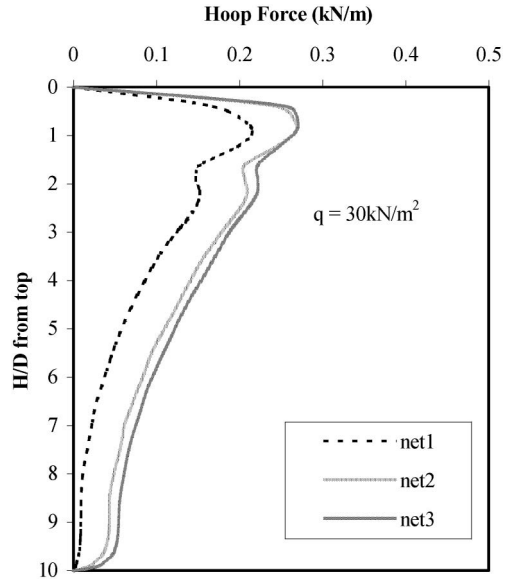

Fig. 9. Variation of hoop force in encasements

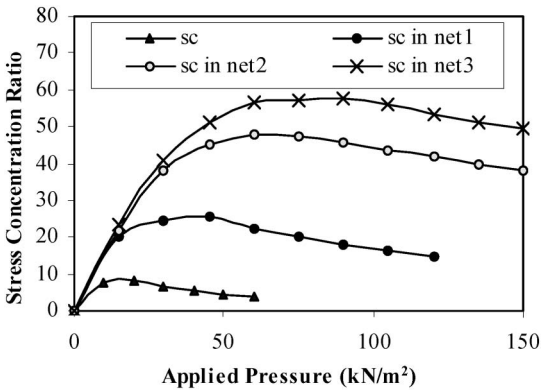

Fig. 10. Stress concentration ratio in column

PARAMETRIC STUDY

An axisymmetric FEM analysis was carried out on a single column stabilized clay bed to bring out influence of various column parameters. Column of 1 m in diameter and 10 m in length was modeled in a clay bed of 20 m thick. The loads of equal increments were applied over an area with diameter equal to 2.5 times the diameter of stone column and incremented at equal time intervals. Each load increment was 10 kN/m^2 and the time interval was 10 days (Fig. 11). The maximum load considered was 200 kN/m^2, which corresponds to load intensity under a circular storage tank of 20 m height.

The parameter chosen for comparison is settlement reduction ratio, which is defined as the ratio of the settlement of treated ground to that of the untreated ground under identical surcharges (Aboshi et al., 1979, Schlosser et al., 1983, Rao and Ranjan, 1988). It is the inverse of the settlement ratio defined by Poorooshasb and Meyerhof (1997). The analysis was done for various L/D ratios, angle of internal frictions of the stone material and the stiffness of geogrids. The influence of these parameters on SRR is elaborately discussed.

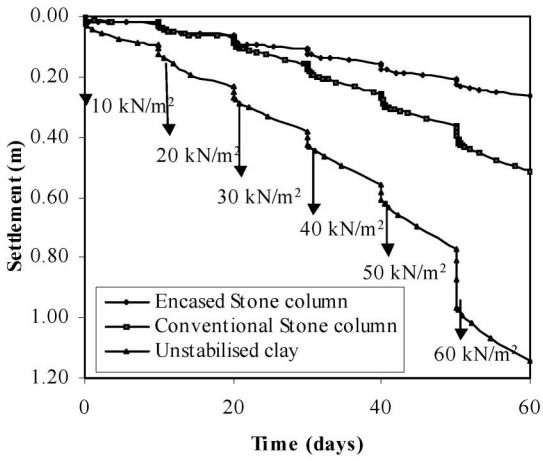

Fig. 11. Load settlement behavior: incremented load of 10 kN/m^2 at an interval of 10 days

Table 7. Parameters used for material modeling

Parameter	Clay	Stone column	Encased stone column
Model	Soft-Soil	Mohr-Coulomb	Mohr-Coulomb
E [kPa]	Not reqd.	24000	48000
ν	0.2	0.35	0.3
γ[kN/m^3]	12	16	16
φ'[°]	30	32–48	32–48
c' [kPa]	6	0.3	0.3
ψ [°]	0	2/3 φ	1/3 φ
k (m/day)	5.94e^{-4}	1	1
λ^*	0.136	Not reqd.	Not reqd.
κ^*	0.054	,,	,,
e_o	1.42	,,	,,

The properties of the materials used for parametric study are shown in Table 7. A constrained modulus of 100 MN/m^2 for the field stone material (Priebe, 1976) is generally used to predict the settlement of stabilized bed theoretically. However, in this study a smaller value of initial tangent modulus (24 MN/m^2) is used because of the very small confining effect offered by soft clay. But in the case of modeling the stone column within the encasement, a higher initial tangent modulus is used to take care of high confining effect (48 MN/m^2). The dilatancy angle of the stone within the encasement is chosen to be half the value (Bauer and Nabil, 1996) of it when used without encasement.

Bulging Behavior

A comparison is made on the behavior of stabilized beds for a load intensity of 60 kN/m^2. Bulging was observed in the stone column and its magnitude was 0.187 m. When an encasement possessing a stiffness of 500 kN/m^2/m was used, bulging reduced to 0.021 m and hoop stress developed was 45.5 kN/m^2/m.

Settlement and Stress Concentration

The settlement for the pressure of 60 kN/m^2 in clay bed of 20 m thick without stone column was 1.14 m. It reduced to 0.5m in stone column bed and 0.26 m in encased stone column bed. The settlement reduction ratio is 0.42 when stone column was used, and it is as low as 0.22 when geogrid was used. The vertical effective stress (mean of the vertical effective stress of the elements just below the loaded area) in unstabilized clay bed at the end of 60 days was observed to be 39 kN/m^2. In the conventional stone column stabilized bed, the stress observed in the stone column was 233 kN/m^2 whereas in clay it was about 12 kN/m^2. In the encased stone column stabilized bed, the stress on stone column was 369 kN/m^2 and in clay, it was 6 kN/m^2. Due to the presence of columns, the stress transferred to clay is less. The stress concentration in the conventional and the encased stone columns was 19 and 61 respectively. Increase in stress concentration was three fold in the encased column.

Pore Pressure Distribution

Figure 12 shows the distribution of excess pore water pressure due to cumulative surcharge pressure of 60 kN/m^2 after the cumulative loading period of 60 days. For identical loading conditions, it is observed that the pore water pressure is less in an encased stone column bed than in stone column stabilised and unstabilised clay beds. One has to distinguish between the settlement reduction due to the enhanced stiffness of the composite soil structure and the settlement acceleration due to the functioning of columns as vertical drains (i.e., acceleration of pore water pressure dissipation).

Han and Ye (2001) proposed modified coefficients of consolidation to account for the effect of stone column-soil modular ratio as against the classical Barron's theory (1948), which ignores the effect of stiffness between the drain well and the surrounding soil, on rate of consolidation. Poorooshasb and Meyerhof (1997) have modified the Barron's equation to include the effect of stress concentration and computed the performance factor with respect to time. Since the coupled effect of deformation and dissipation of pore water is incorporated in PLAXIS FEM code which uses BIOT's (1941) system of differential equations solved by integration over time, the stress concentration effect is automatically taken care of in the present analysis. It is observed from Fig. 12 that the pore water pressure distribution is concentrated below foundation in the unstabilized bed, whereas in the encased stone column and in the conventional stone column stabilized bed, the concentration of pore water pressure is distributed to deeper depths and the intensity is far less than unstabilised condition.

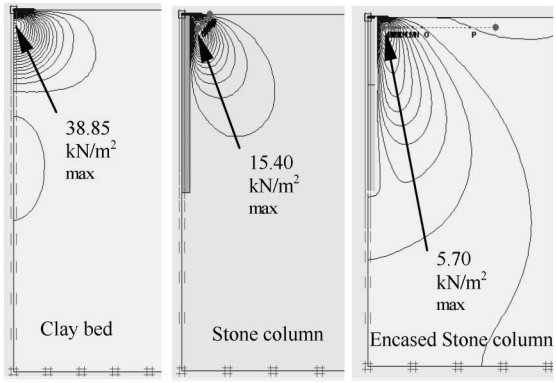

Fig. 12. Excess pore water contours under cumulative surcharge pressure of 60 kN/m^2

L/D ratio on SRR for Stone Column

Variation of SRR for different pressures is presented in Fig. 13. When the pressure on the bed is less, SRR is less and around 0.4 for a pressure of 50 kN/m^2. However, SRR increases with pressure for all the L/D ratios and the SRR is 0.6 for a pressure increase of 200 kN/m^2.

As the L/D ratio increases, SRR reduces. But the increase in the length of column beyond $L/D = 7.5$ does not contribute to the settlement reduction. However, the rate of reduction in SRR is decreased and reached almost to a constant value for L/D more than 10. Narasimha Rao (2000) has also reported that a slenderness ratio (L/D) of 5 to 10 is ideal and increase in L/D ratio does not contribute to either load carrying capacity or reduction in settlement.

L/D ratio on SRR for Encased Stone Column

A behavior as said above was observed in the encased stone column also. As the L/D ratio increases, SRR reduces, but it is effective up to $L/D = 7.5$ against 10 for the conventional stone column. Further increase in the length of column does not contribute to the settlement reduction. The SRR at different pressures is presented in Fig. 14. For an applied pressure of 100 kN/m^2, SRR varies from 0.65 to 0.55 (Fig. 13) for L/D varying from 5 to 10 in case of a stone column stabilized bed. In the case of

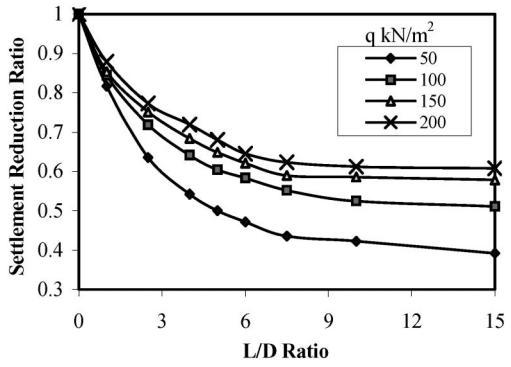

Fig. 13. L/D vs. SRR for stone column

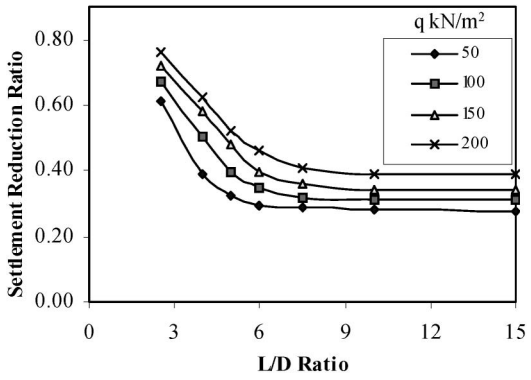

Fig. 14. L/D vs. SRR for encased stone column

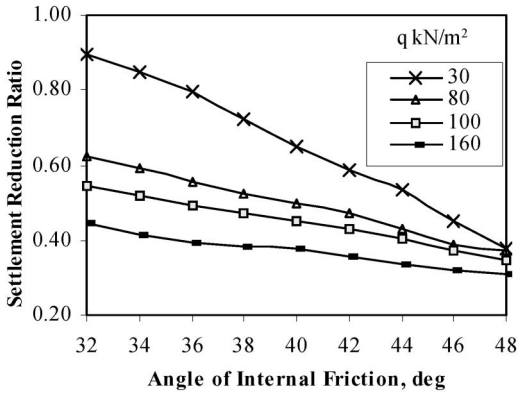

Fig. 15. Angle of internal friction vs. SRR

an encased stone column, SRR varies from 0.40 to 0.30 (Fig. 14), which means, the settlement is 50% of the conventional stone column bed.

ϕ vs. SRR (stone column)

As the angle of internal friction of stone increases, the settlement reduction ratio decreases and is observed to be the same for all load intensities. However, when the applied load is low and column is very loose, e.g. for $\phi = 32°$, the settlement reduction ratio is almost 1 (Fig. 15), which implies that a loose material is less stiff and does not contribute much to load carrying capacity. As the

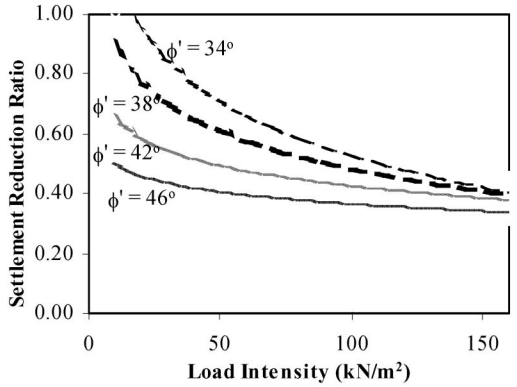

Fig. 16. Load intensity vs. SRR for a stone column

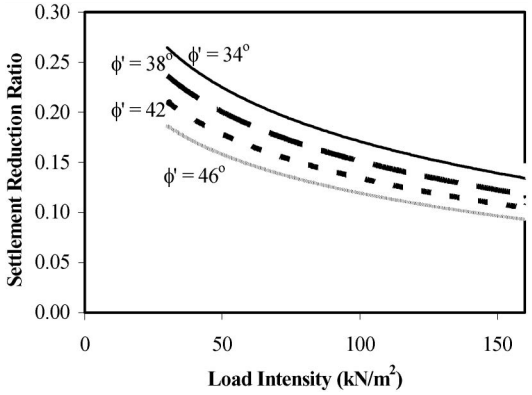

Fig. 17. Load intensity on SRR for encased column

load intensity increases, the SRR decreases. As indicated in Fig. 16, SRR is less in the well packed column, ($\phi = 46°$) and is almost 0.4 for the pressures between 50 kN/m^2 and 150 kN/m^2. But for $\phi = 34°$, the SRR is 0.8 for the pressure of 50 kN/m^2 and reduces to 0.5 for the pressure of 150 kN/m^2.

ϕ vs. SRR (encased stone column)

Unlike in stone column, SRR is less affected in encased column by the angle of internal friction of column material, which can be seen in Fig. 17. The SRR for different stone column materials enclosed with geogrids of varying axial stiffness is plotted in Fig. 18. The SRR for the column material with lesser angle of internal friction ($\phi = 34°$) is 0.9 in conventional stone column, but is only 0.275 in the case of encased stone column. This proves that the encasement is very effective for weak column material. When the stiffness of geogrid material is high, SRR is small. SRR as small as 0.1 is obtained for the modulus of encasement of 3000 kN/m^2/m irrespective of angle of shearing resistance of stone material. This indicates that the settlement of soft clay bed can be reduced to 10% by encased stone column stabilization.

Influence of stiffness of geogrid

As the stiffness of geogrid material (E_s) increases, SRR reduces, but beyond a certain value, further increase in

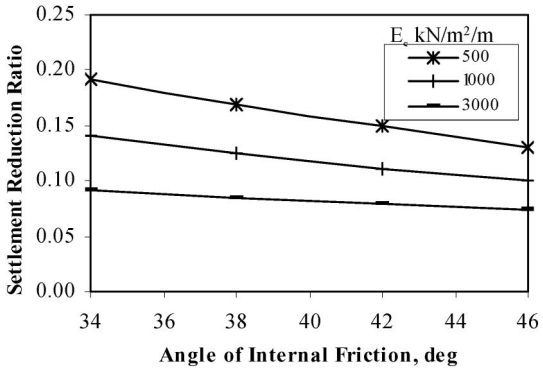

Fig. 18. Angle of internal friction vs. SRR

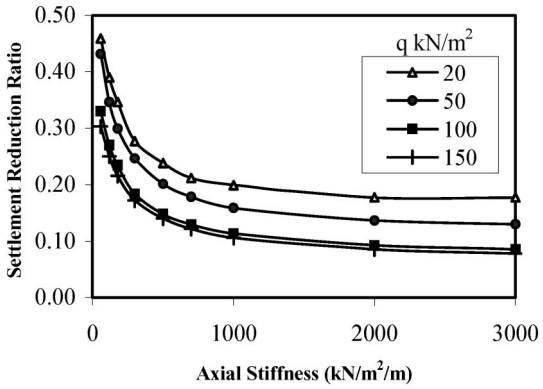

Fig. 19. Stiffness of geogrid on SRR for different pressures

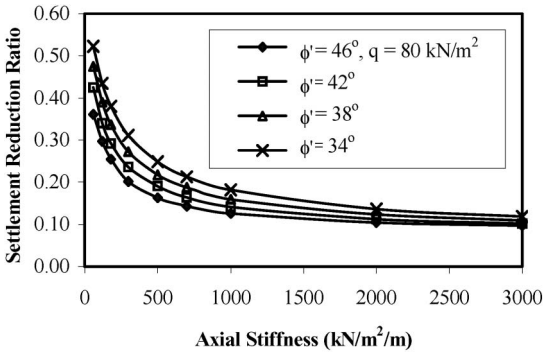

Fig. 20. SRR vs. Stiffness of geogrid for different ϕ

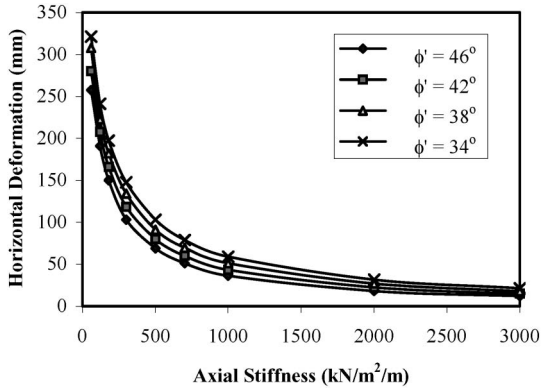

Fig. 21. Horizontal displacement vs. Stiffness of geogrid for different ϕ' values

the stiffness of geogrid is not effective. For a load intensity of 20 kN/m^2, it can be seen from Fig. 19 that as the stiffness value increases from 60 to 1000 kN/m^2/m, SRR reduces from 0.45 to 0.2, but when the stiffness is doubled, say 2000 kN/m^2/m, the ratio is just 0.17. The trend is the same for higher pressures also, but SRR is less for higher pressures. For the conditions presented, the increase in stiffness of geogrid beyond certain value is not effective in reducing the SRR. Therefore, it can be said that when an appropriate geogrid material is used the SRR value is reduced effectively and it will be cost effective.

Almost similar trend is observed when the column material has different angle of internal friction as shown in Fig. 20. It is seen that higher the ϕ value, the lesser the SRR for a given stiffness of the geogrid. The angle of shearing resistance of the material is also contributing to some degree in reducing the SRR. Therefore, column material needs good compaction so that higher ϕ value is achieved, which will enhance the efficiency of encased stone column in reducing the SRR. The importance of higher value of internal friction in stone column material (adequate compaction of stone column) is further strengthened through the variation of horizontal deformation of column and hoop forces with respect to axial stiffness of geogrid material (Figs. 20 and 21). With increase in angle of shearing resistance, the deformation of column is reduced for an axial stiffness of the geogrid. But the effect of axial stiffness is highly pronounced than the angle of shearing resistance of stone column material as seen in Fig. 21. However, the stiffness of more than 2000 kN/m^2/m is not effective for the conditions of the column analysed in this study. Similarly, the hoop force in the geogrid is less if the angle of shearing resistance in the column is more and the mobilized hoop force is almost constant despite the increase in axial stiffness. The maximum hoop forces for all the field models were observed to be at about 0.75D from the column top.

CONCLUSIONS

Based on the observation of experimental investigation on model encased stone column stabilized bed and detailed parametric study through FEM analysis following conclusions are drawn.

1. Stone columns improved the load carrying capacity of the stabilized bed. As the length of the stone column increases, there is an increase in the load carrying capacity. Column has shared higher load by the passive resistance against bulging. Bulging is observed effectively at the top 4D of the column.
2. Encasing the stone column with geogrids improved the load carrying capacity of the stabilized bed appreciably. The stiffer the geogrid is the higher is the load carrying capacity.

3. The load-settlement curves obtained from finite element analyses compare well with experimental curves suggesting that material models viz. Soft soil, Mohr Coulomb and geogrid models used in the FEM analyses are effective in idealising the behaviour of soft clay, stone column and encasement respectively.
4. Numerical studies confirmed the bulging mechanism of stone column. The bulging of stone column is effective up to the depth of 4 times the diameter of the column, which is in conformity with classical theories of Hughes and Withers (1974) and Greenwood (1970) and the present experimental study.
5. The mobilised hoop force in the geogrid material increases with increase in surcharge pressure. Initially, the hoop force is mobilised over the top $1D$ depth, and as the pressure increases, the hoop force is mobilised over the length of column apart from increase in its magnitude. Further, the hoop stress is always maximum at $1D$ depth of the column for the parameters analysed in this study.
6. Encasing the stone column increases the stress concentration on the column, thereby reducing the load on clay, consequently reducing the settlement. The parametric study shows that the settlement reduction ratio in the encased stone column bed is about 50% of stone column bed for identical conditions.
7. The stress concentration factor increased with the stiffness of encasement and is always higher than in conventional stone column irrespective of applied pressure.
8. The parametric study shows that the increase in stiffness of encasement reduces the settlement, but when the stiffness is increased beyond 2000 $kN/m^2/m$, the contribution to settlement reduction ratio becomes insignificant for the conditions analysed in this study.
9. As the L/D ratio of column increases, settlement reduces and if the L/D ratio is more than about 10, it does not contribute much to settlement reduction.
10. The angle of shearing resistance of column material also affects the SRR of encased stone column but not to the extent of stiffness of encasing material. Efficiency of encased stone column is higher if the column material is compacted well to achieve high angle of shearing resistance.

REFERENCES

1) Aboshi, H., Ichimoto, E., Enoki, M. and Haraka, K. (1979): The Compozer—A method to improve characteristics of soft clays by inclusion of large diameter sand columns, *Proc. International Conference on Soil Reinforcement: Reinforced Earth and other Techniques*, **1**, 211–216.
2) Adayat, T. and Hanna, A. M. (2005): Encapsulated stone columns as a soil improvement technique for collapsible soil, *Ground Improvement*, **9**(4), 137–147.
3) Alexiew, D., Brokemper, D. and Steve, L. (2005): Geotextile Encased Columns (GEC): Load capacity, geotextile selection and predesign graphs, *Geofrontiers 2005, GSP 131 Contemporary Issues in Foundation Engineering*, 1–14.
4) ASTM: *D4767–04—Consolidated Undrained Triaxial Compression Test for Cohesive Soils*.
5) ASTM: *D6637–01—Determining Tensile Properties of Geogrids by the Single or Multi-Rib Tensile Method*.
6) Balaam, N. P. and Poulos, H. G. (1983): The Behavior of foundations supported by clay stabilized by stone columns, *Proc. Specialty Sessions, VII European Conference on SMFE*, **2**.
7) Barron, R. A. (1948): Consolidation of fine-grained soils by drain wells, *Transactions of the American Society of Civil Engineers*, **113**, paper 2346, 718–724.
8) Bauer, G. E. and Nabil, A. J. (1996): Laboratory and analytical investigation of sleeve reinforced stone columns, *Geosynthetics: Application, Design and Construction*, 463–466.
9) Biot, M. A. (1941): General theory of three-dimensional consolidation, *J. Appl. Phys.*, **12**, 1941a, 155–165.
10) Bouassida, M. and Hadhri, T. (1995): Extreme load of soils reinforced by columns: The case of an isolated column, *Soils and Foundations*, **35**(1), 21–35.
11) Burland, J. B. (1965): The yielding and dilation of clay, *Géotechnique*, **15**, 211–214.
12) Datye, K. R. and Nagaraju, S. S. (1981): Design approach and field control for stone columns, *Proc. 10th International Conference on Soil Mechanics and Foundation Engineering*, 637–640.
13) Deshpande, P. M. and Vyas, A. V. (1996): Interactive encased stone column foundation, *6th International Conference and Exhibition on Piling and Deep Foundation*, DFI'96, ISSMFE, 1–19.
14) Greenwood, D. A. (1970): Mechanical improvement of soils below ground surface, *Conference on Ground Engineering*, Institution of Civil Engineering, 11–22.
15) Han, J. and Ye, S. L. (2001): Simplified method for consolidation rate of stone column reinforced foundations, *J. Geotechnical and Geoenvironmental Engg*, **127**(7), 597–603.
16) Hughes, J. M. O. and Withers, N. J. (1974): Reinforcing of soft cohesive soils with stone columns, *Ground Engineering*, **7**(3), 42–42 and 47–49.
17) Katti, R. K., Katti, A. R. and Naik, S. (1993): *Monograph to Analysis of Stone Columns with and without Geo-synthetic Encasing*, CBRI publication, New Delhi.
18) Lee, J. S. and Pande, G. N. (1998): Analysis of stone column reinforced foundations, *Int. J. Numerical and Analytical Meth in Geomech.*, **22**, 1001–1020.
19) Madhav, M. R., Miura, N. and Alamgir, M. (1994): Analysis of granular column reinforced ground, *5th International Conference on Geotextile, Geomembranes and Related Products*.
20) Meyerhof, G. G. and Sastry, V. V. R. N. (1978): Bearing capacity of piles in layered soils, part I and II, *Canadian Geotechnical Journal*, **15**, 171–189.
21) Mitchell, J. K. and Huber, T. R. (1985): Performance of a stone column foundation, *Journal of Geotechnical Engineering*, **111**, 205–223.
22) Narasimha, Rao. S. N. (2000) Studies on groups of stone column in soft clays, *Symposium on Ground Improvement Techniques For Practicing Engineers*, India, 84–93.
23) Nayak, N. V. (1983): Recent advances in ground improvements by stone volumn, *Proc. Indian Geotechnical Conference*, **1**, V–19.
24) Poorooshasb, H. B. and Meyerhof, G. G. (1997): Consolidation settlement of rafts supported by stone columns, *Journal of Geotechnical Engineering*, 83–92.
25) Priebe, H. J. (1976): An evaluation of settlement reduction in soil improved by vibroreplacement (en alemán), *Bautechnik*, (53), 160–162.
26) Raithel, M., Kirchner, A., Schade, C. and Leusink, E. (2005): Foundation of constructions on very soft soils with geotextile encased columns—State of the Art, *Geofrontiers 2005*, GSP 131 Innovations in grouting and soil improvement, 1–11.
27) Rao, B. and Ranjan, G. (1988): Closure of the paper Settlement analysis of skirted granular piles, *Journal of Geotechnical Engineering Division*, ASCE, **114**, 729–736.
28) Schlosser, F., Jacobsen, H. U. and Juran, I. (1983): General report

on soil reinforcement, *Proc. 8th European Conference on SMFE*, **3**, 1159–1180.
29) Short, R. D., Prashar, Y. and Metcalf, B. (2005): Repairing a railway spur roadbed failure using geotextile encased columns, *TRB 2005 Annual Meeting Report*.
30) Sivakumar, V., Mckelvey, D., Graham, J. and Hughes, D. (2004): Triaxial tests on model sand columns in clay, *Canadian Geotechnical Journal*, **41**, 299–312.
31) Van Impe, W. Y. and De Beer, E. (1983): Improvement of settlement behaviour of softy layers by means of stone columns, *Proc. 8th International Conference on SMFE*, Helsinki, 309–312.
32) Vermeer, P. A. and Brinkgreve, R. B. J. (1998): *Plaxis Finite Element Code for Soil and Rock Analyses*, Rotterdam, Balkema.